X-641-67-308

NASA TM X- 55819

GEOMAGNETIC EULER POTENTIALS*

DAVID STERN

GPO PRICE $ ______

CFSTI PRICE(S) $ ______

Hard copy (HC) 3.00

Microfiche (MF) .65

ff 653 July 65

N67-29995 (ACCESSION NUMBER)

16 (PAGES)

TMX-55819 (NASA CR OR TMX OR AD NUMBER)

(THRU) 1

(CODE) 13

(CATEGORY)

FACILITY FORM 602

JUNE 1967

NASA

GODDARD SPACE FLIGHT CENTER

GREENBELT, MARYLAND

*Presented 16 June 1967 at the Conjugate Point Symposium, Boulder, Colorado.

Geomanetic Euler Potentials

David Stern

Laboratory for Theoretical Studies
Goddard Space Flight Center
Greenbelt, Maryland ~~20771*~~

It has been known for many years that any solenoidal field - for instance, a magnetic field $\underline{B}$ - can be represented as the cross product of the gradients of two scalars, usually denoted by α and β

$$\underline{B} = \nabla\alpha \times \nabla\beta \tag{1}$$

In fact it was Euler (1769), who first used this representation; figure 1 is taken from one of his works. In this figure, u, v and w are the cartesian components of the field vector, and one sees - apart from the irrelevant functions Γ, Δ and Σ, and from the fact that Euler used no special notation for partial derivatives - that they are given by the cross product of the gradients of the scalars F and G. It therefore appears appropriate to refer to such scalars as <u>Euler potentials</u>.

The advantage of Euler potentials is that, by definition, $\nabla\alpha$ and $\nabla\beta$ are both perpendicular to the field vector $\underline{B}$. Because of this property, $\underline{B}$ is tangential to surfaces of constant α and of constant β, and the intersections of pairs of such surfaces yield field lines. In other words, each field line is labeled by a pair of constant values, assumed by the

---

*Presented 16 June, 1967 at the Conjugate Point Symposium, Boulder, Colorado.

functions α and β which are conserved on it.

In classical electrodynamics, field lines play a relatively minor role, and for this reason the study of Euler potentials has been neglected for a long time. On the other hand, field lines are important in plasma physics and in the motion of charged particles, and indeed, it was in this connection that Euler potentials were reintroduced during the last decade, in theoretical work by Northrop and others.

The purpose of this work is to review some recent results on geomagnetic Euler potentials. It will be shown that they can serve not only as a purely theoretical tool but as a practical one, as something that can be expressed and used in a similar manner as can, for instance, the geomagnetic scalar potential V .

The difficulty in trying to do so arises from the fact that the representation is nonlinear, since it contains products of derivatives of α and β. Because of this nonlinearity, Euler potentials are in general hard to obtain explicitely, except for certain fields with a high degree of symmetry. One may not, in such a derivation, resolve the field into simple components and then add up their Euler potentials, because superposition does not exist in this case.

One may, however, make use of the fact that the geomagnetic field - to which we now restrict the discussion - is not too different from a dipole field, for which Euler potentials are readily found. Denoting by a the earth's radius, by g_1^0 the dipole coefficient in the spherical harmonic expansion of the scalar potential V and by subscript zero any quantity associated with the dipole field, these are (one choice out of many possible)

$$\alpha_0 = a\, g_1^0\, (a/r)\, \sin^2\theta$$

$$\beta_0 = a\, \phi \tag{2}$$

One notes that β_0 is proportional to the azimuth angle ϕ, signifying that dipole field lines lie in meridional planes, whereas α_0 is proportional to $\sin^2\theta/r$, a quantity which is known to be conserved along dipole field lines. Using the complete spherical harmonic expansion of γ, one can now obtain a first-order correction which, when added to the dipole Euler potentials of equation (2), yields a better approximation to α and β of the geomagnetic field. The correction turns out to have an analytical form and to be fairly simple, but its derivation is too lengthy to be included here. Details may be found in the work of Stern (1967), and the method is also related to that of Pennington (1967).

One possible application of the results is the labeling of conjugate points, as given in Figure 2, which shows a map of α and β on the earth's surface. As has been noted, each field line is characterized by a pair of constants, which are the values of α and β on it. A pair of conjugate points, threaded by the same field line, is therefore identified on this map as a pair of points having the same values of α and β.

The map shown here is based on first-order potentials, and is accurate within about 2 degrees. The next step would be the derivation of more accurate values, not only on the earth's surface but in the entire surrounding space. In principle, this could have been accomplished by carrying the approximation to its second order, which also has analytical form. In fact, such a derivation and the results it gives are lengthy and inconvenient, so that it appears to be better to evaluate the higher correction numerically. This approach also appears to be useful for including in the model the effects of a ring current, but the details are beyond the scope of this brief review.

Another application concerns the <u>external magnetosphere</u>. For this region, models have been developed (Mead, 1964) in which the expansion of the scalar potential Υ includes terms increasing with distance, and in general, among these terms, two - involving the coefficients $\bar{g}_1^0$ and $\bar{g}_2^1$ - are by far the most important.

Starting from a model including only the dipole part and the above two terms, on can derive first-order Euler potentials

$$\alpha a = [g_1^0 (a/r) - \tfrac{1}{2} \bar{g}_1^0 (r/a)^2] \sin^2\theta + \\ + 2\sqrt{3} \; \bar{g}_2^1 (r/a)^3 \; [(\sin\theta/7) - (\sin^3\theta/3)] \; \cos \phi \tag{3}$$

$$\beta a = \phi - (\sqrt{3}/7) \; (\bar{g}_2^1/g_1^0) \; (r/a)^4 \; \sin^{-1}\theta \; \sin \phi \tag{4}$$

The features of this model are shown in figure 3, giving its lines of constant α (which in this case are also field lines) in the noon-midnight meridian. As can be seen, the model fits surprisingly well our concepts of the magnetosphere - probably better so than the current-free model from which it was derived. Because an approximation was used in its derivation, it is not current free, and it is interesting to note that it has 3 neutral points - two in front and one in the rear, where one may perhaps splice onto it a neutral sheet.

Figure 4 gives the equatorial cross section of the model, with solid lines giving lines of constant β and broken ones those of constant α. One can observe here how field lines are swept backwards, a result also obtained from other models.

The remainder of this work will discuss the equations of drift shells, that is, of surfaces traced by trapped particles in their adiabatic motion. As will be seen, such equations are most naturally expressed by means of Euler potentials.

Because drift shells are tangential to field lines, their equations have the form

$$f(\alpha,\beta) = 0 \tag{5}$$

or

$$\alpha = g(\beta) \tag{6}$$

The entire collection of drift shells in the geomagnetic field can be characterized by two parameters, depending on the associated adiabatic invariants of each shell. In particular, one may choose for such parameters the field intensity B_m at the mirror point and the integral along a field line

$$I = \int_{B \leq B_m} \sqrt{1 - B/B_m}\, d\ell \tag{7}$$

The entire family may thus be described by an equation of the form

$$\alpha = G(\beta, I, B_m) \tag{8}$$

In a dipole field, as was seen in equation (2), β_0 is proportional to the azimuth angle ϕ and, due to axial symmetry, does not appear in the preceding equation. Equation (8) may therefore be rewritten in the form

$$\alpha_0 = \frac{\text{constant}}{L(I,B_m)} \tag{9}$$

where $L(I,B_m)$ is some function of the parameters I and B_m and is in fact the same as the function L introduced by McIlwain (1961) and widely used. In a perturbed dipole field, there will be an additional "shell splitting" correction term, which brings the equation to the form

$$\alpha = \frac{\text{constant}}{L(I,B_m)} + G_1(r,\theta,\phi,B_m) \tag{10}$$

This term gives the next step beyond using L alone to label drift shells (as experimenters nowadays do), since it describes the variation between shells having the same value of L. An approximation to G_1 may be obtained by using first-order Euler potentials (Stern, to be published); the results are equivalent to those obtained by Pennington (1961), who used a perturbation technique to obtain approximate magnetic shells for the geomagnetic field.

Shell splitting increases with departure from axial symmetry and is thus most pronounced in the external magnetosphere. It is, therefore, most instructive to examine some results on the deformation and splitting of drift shells obtained with the previously described magnetospheric model, for which the first-order shell splitting function is readily found.

In this model, we launched particles with various pitch angles from given points in the equatorial plane, and asked where they would pass this plane on the opposite side of the earth. Figure 5 shows the nightside intersections of particles starting from 7 earth radii on the noon side. Two methods were used - a perturbation method using a first-order approximation to G_1 , and an exact method using adiabatic invariants. It is evident that the two methods agree quite well, and also that the drift shells depart considerably from axial symmetry.

Next we did something requiring more accuracy but also more interesting - we let the initial pitch angle of each particle be scattered downwards by one degree, and examined, by how much did such scattering cause the midnight intersection to move radially. The results are given in Figure 6, and one notes that the agreement between the two methods is only qualitative, this being a more sensitive test. With either method, however, the interesting fact emerges that such scattering causes particles with pitch angles around 70° to move further radially than those with either larger or smaller pitch angles. If, as has been suggested, the combination of asymmetry and small angle scattering is an important mechanism in transporting radiation-belt particles across field lines, then the preceding would imply that such transport is strongly pitch-angle dependent, being most efficient for pitch angles around 70°.

In conclusion, it appears that Euler potentials have considerable practical use, for investigation of conjugacy and for broader purposes. In the future, it is hoped the avenues sketched out here will all be fully explored, and Euler potentials will become one of the standard tools of the trade.

References

Euler, L. (1769), Sectio Secunda de Principiis Motus Fluidorum, Novi Comentarii Acad. Sci. Petropolitanae 14, 270; reprinted in Leonhardi Euleri Opera Omnia, Series II, vol. 13, p. 73, published by the Swiss Society for Natural Sciences, 1955.

McIlwain, C. E. (1961), Coordinates for mapping the distribution of Magnetically Trapped Particles, J. Geophys. Research 66, 3681.

Mead, G. D. (1964), Deformation of the Geomagnetic Field by the Solar Wind, J. Geophys. Research 69, 1181.

Pennington, R. H. (1961), Equation of a charged Particle Shell in a Perturbed Dipole Field, J. Geophys. Research 66, 709.

Pennington, R. H. (1967), Derivation of Geomagnetic Shell Equations, Air Force Weapons Laboratory Report AFWL-TR-66-152.

Stern, D. P. (1967), Geomagnetic Euler Potentials, to be published in J. Geophys. Research.

Captions to Figures

Figure 1 - No caption

Figure 2 - Lines of constant first-order Euler potentials on the earth's surface. Plotted are β/a in 10-degree intervals, as well as (ag_1^0/α) - the quantity which in a dipole field equals the equatorial crossing distance in earth radii - for the values (increasing with distance from the geomagnetic equator, which is also shown) 1, 1.05, 1.1, 1.25, 1.5, 1.75, 2, 2.5, 3, 4, 5 and 10 earth radii.

Figure 3 - Lines of constant α in the noon-midnight meridian of the first-order magnetospheric model. Values given are those of (ag_1^0/α).

Figure 4 - Lines of constant β (solid) and of constant α (broken) in the equatorial plane of the first-order model magnetosphere. Values given are those of (ag_1^0/α).

Figure 5 - The equatorial crossing distance in earth radii on the midnight meridian, for particles starting with various pitch angles on the equator at 7 R_e, on the sunward side.

Figure 6 - The night-time radial displacement in earth radii resulting from a one-degree pitch angle scattering, for particles starting with various pitch angles on the equator at 7 R_e, on the sunward side.

SCHOLION 2

49. Ex solutione problematis, dum per gradus ad aequationem propositam sumus progressi, casum, quo fluidi densitas q est constans et prima aequatio ita se habet

$$\left(\frac{du}{dx}\right)+\left(\frac{dv}{dy}\right)+\left(\frac{dw}{dz}\right)=0,$$

resolvere poterimus, quod eo magis est notandum, quod huius solutionem ex generali, quam dedimus, derivare non licet. Quamquam autem hic tres tantum variabiles x, y et z considerantur, tamen nihil impedit, quominus in solutione ibi data etiam quartum t introducamus, eam quasi constantem spectando. Sumtis ergo pro lubitu duabus functionibus F, G quatuor variabilium x, y, z et t, ex iis ternae celeritates u, v et w ita determinabuntur, ut sit

$$u=\left(\frac{dF}{dy}\right)\left(\frac{dG}{dz}\right)-\left(\frac{dF}{dz}\right)\left(\frac{dG}{dy}\right)+\Gamma:(y,z,t)$$

$$v=\left(\frac{dF}{dz}\right)\left(\frac{dG}{dx}\right)-\left(\frac{dF}{dx}\right)\left(\frac{dG}{dz}\right)+\Delta:(x,z,t)$$

$$w=\left(\frac{dF}{dx}\right)\left(\frac{dG}{dy}\right)-\left(\frac{dF}{dy}\right)\left(\frac{dG}{dx}\right)+\Sigma:(x,y,t),$$

ubi totum momentum iterum in eo est situm, quod cuivis membro cuiusque formae in reliquis respondeat aliquod, quod cum eo datum factorem habeat communem et signo contrario sit affectum. Totus autem hic casus, quo densitas fluidi est quantitas constans, meretur, ut seorsim diligentius evolvatur,

Figure 1

LINES OF CONSTANT α AND β

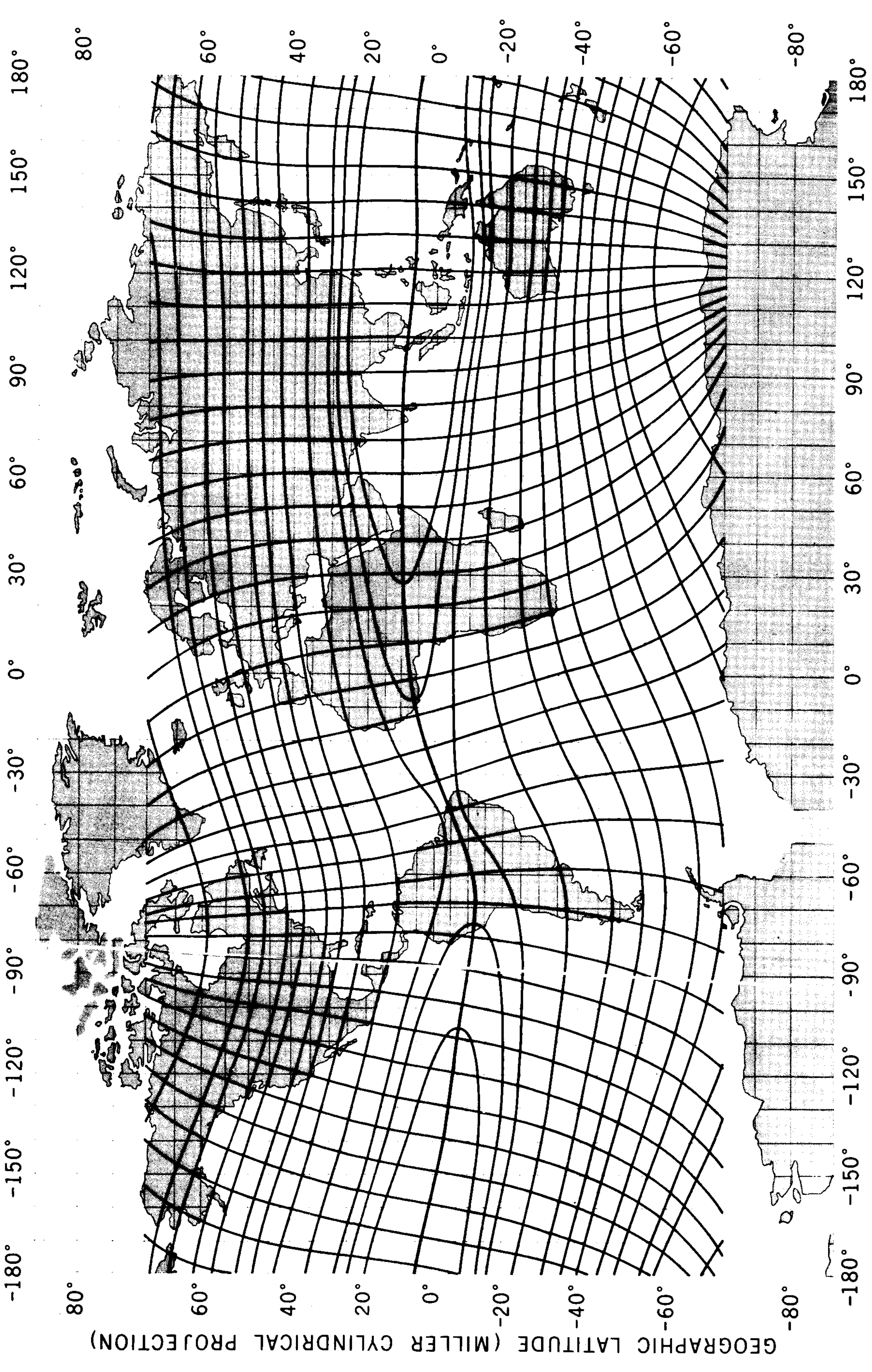

Figure 2

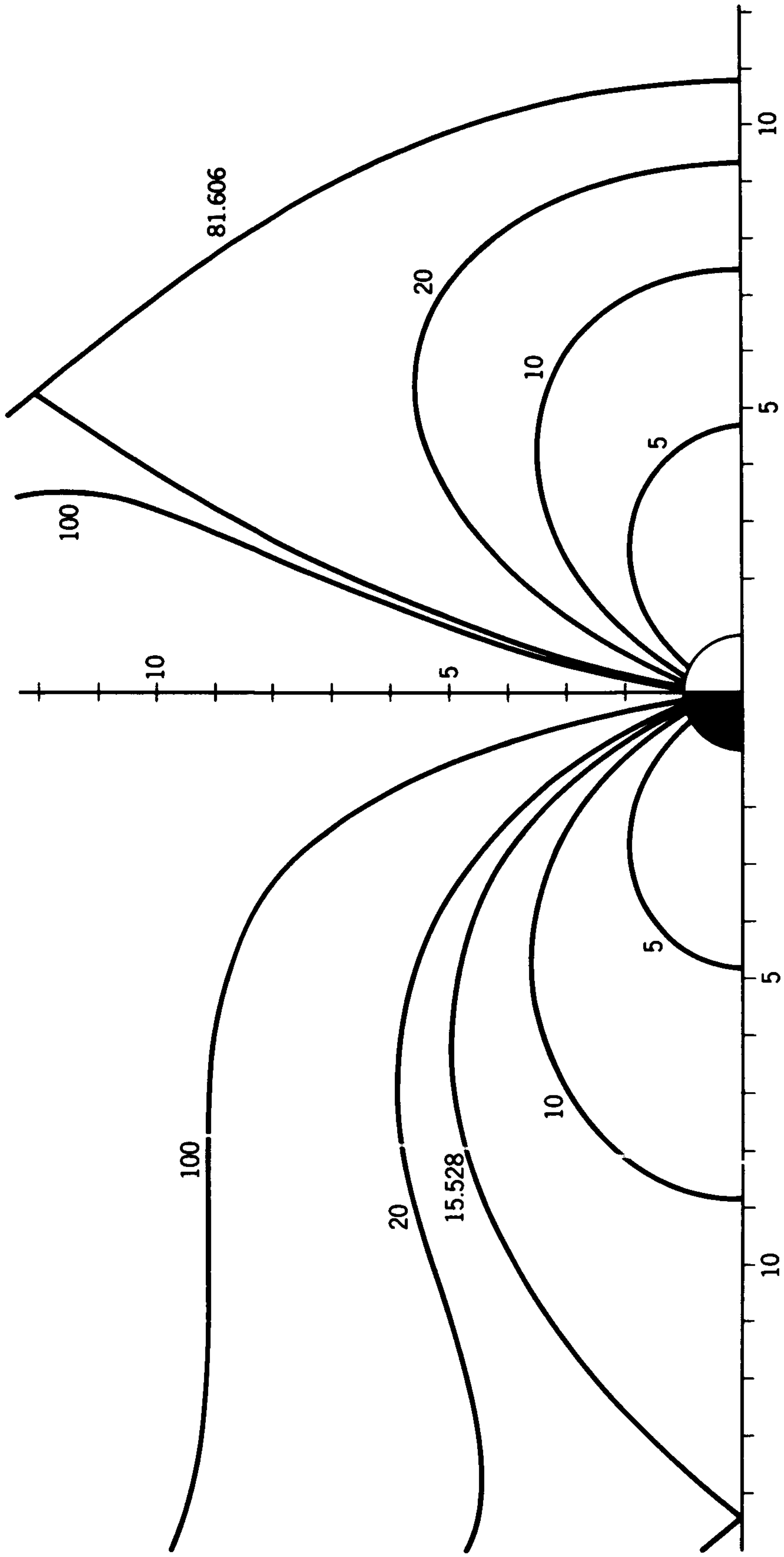

Figure 3

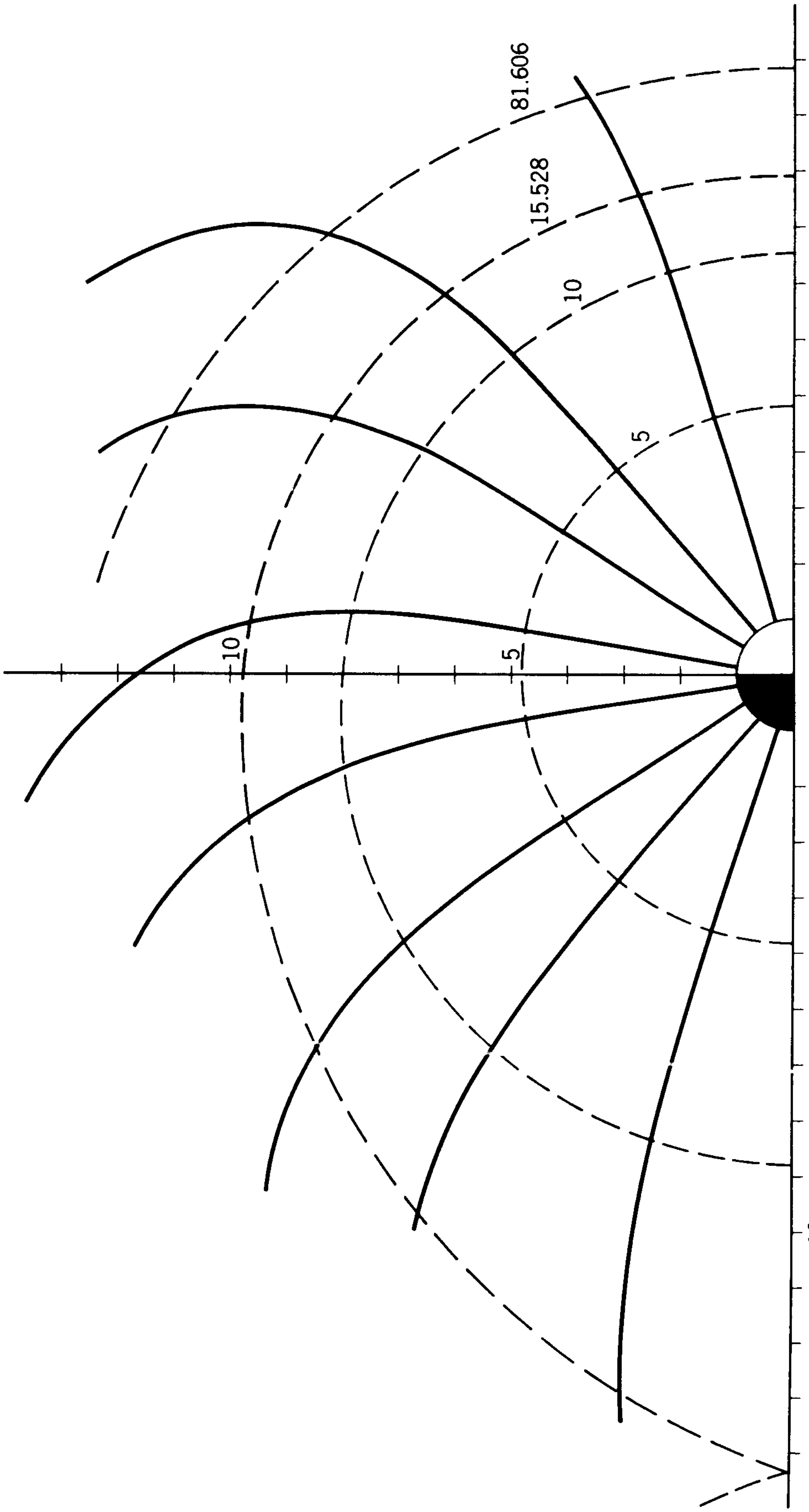

Figure 4

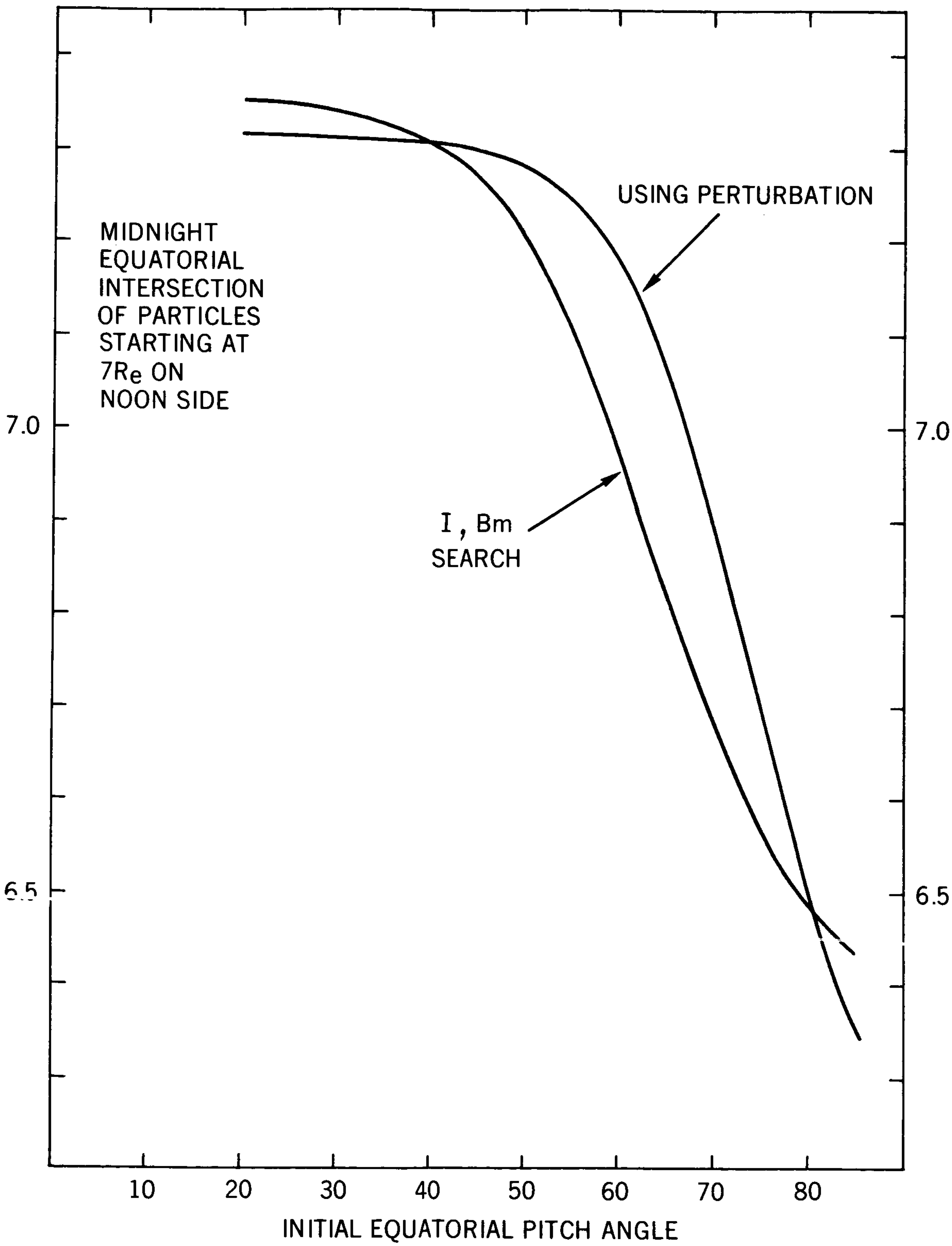

MIDNIGHT
EQUATORIAL
INTERSECTION
OF PARTICLES
STARTING AT
7Re ON
NOON SIDE
USING PERTURBATION
I, Bm
SEARCH
7.0
6.5
7.0
6.5
10
20
30
40
50
60
70
80
INITIAL EQUATORIAL PITCH ANGLE

Figure 5

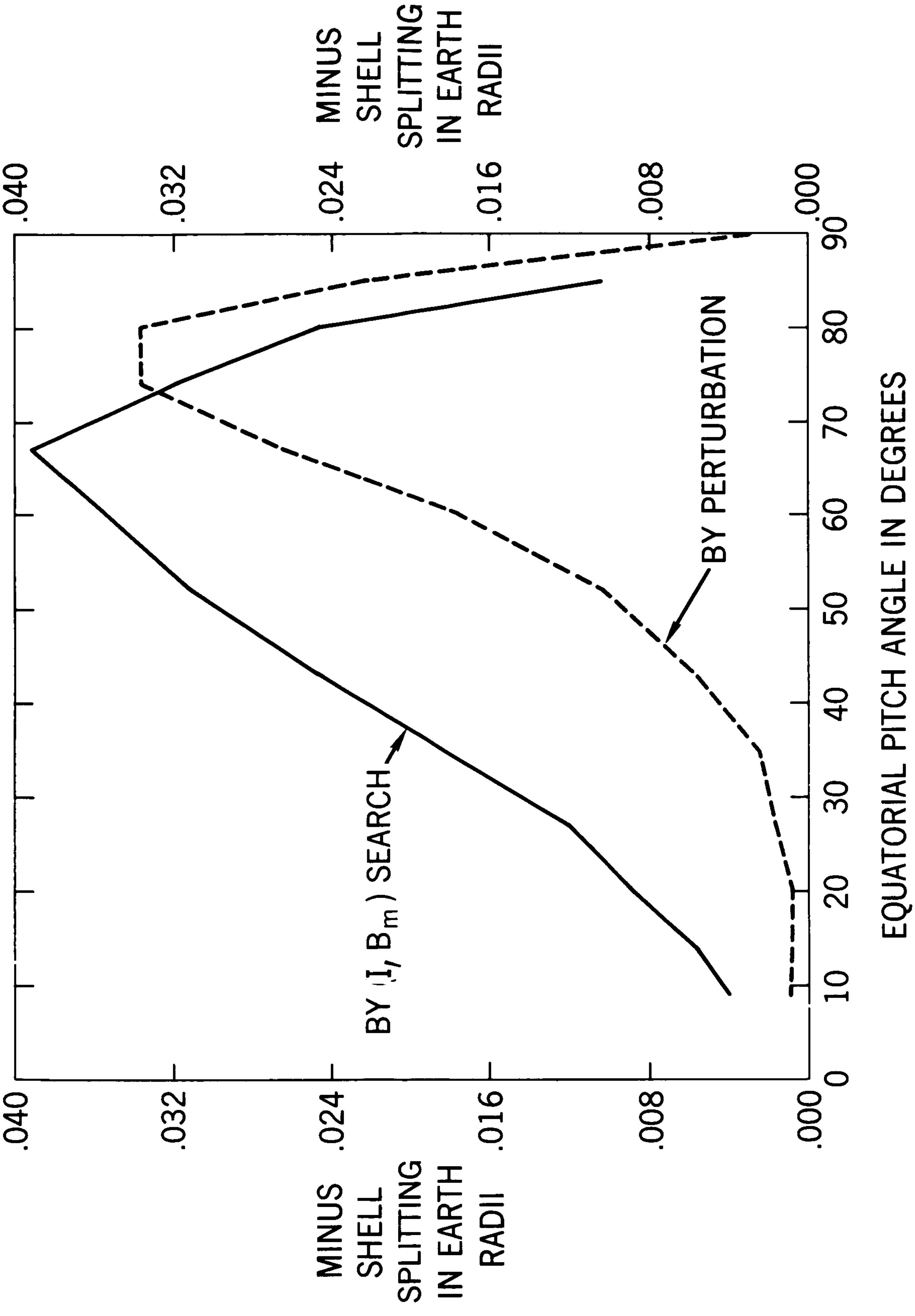

MINUS SHELL SPLITTING IN EARTH RADII
.040
.032
.024
.016
.008
.000
0
10
20
30
40
50
60
70
80
90
EQUATORIAL PITCH ANGLE IN DEGREES
BY PERTURBATION
BY (I, B_m) SEARCH
MINUS SHELL SPLITTING IN EARTH RADII

Figure 6